

# Nanoscale

Accepted Manuscript



This is an *Accepted Manuscript*, which has been through the Royal Society of Chemistry peer review process and has been accepted for publication.

*Accepted Manuscripts* are published online shortly after acceptance, before technical editing, formatting and proof reading. Using this free service, authors can make their results available to the community, in citable form, before we publish the edited article. We will replace this *Accepted Manuscript* with the edited and formatted *Advance Article* as soon as it is available.

You can find more information about *Accepted Manuscripts* in the [Information for Authors](#).

Please note that technical editing may introduce minor changes to the text and/or graphics, which may alter content. The journal's standard [Terms & Conditions](#) and the [Ethical guidelines](#) still apply. In no event shall the Royal Society of Chemistry be held responsible for any errors or omissions in this *Accepted Manuscript* or any consequences arising from the use of any information it contains.

# Suspended single-walled carbon nanotube fluidic sensors

B. H. Son, Ji-Yong Park, Soonil Lee, and Y. H. Ahn\*

*Department of Physics and Department of Energy Systems Research, Ajou University, Suwon 443-749, Korea*

In this paper, we demonstrate the fabrication of liquid flow sensors employing partially suspended single-walled carbon nanotubes (SWNTs). We have found that the sign of the conductance change in SWNT flow sensors is not influenced by the direction of water flow for both supported and suspended devices. Therefore, the streaming potential is not the principal mechanism of SWNT sensor response. Instead, the conductance change is more likely due to a reduction in cation density in the electrical double layer, whose equilibrium conditions are determined by the liquid flow rate. More importantly, we have found that the sensitivity of suspended SWNT devices is more than 10 times greater than that of supported SWNT devices. A reduced screening effect and an increase in effective sensing volume are responsible for the enhanced sensitivity, which is consistent with the ion depletion model. We also have measured conductance as a function of gate bias at different flow rates and have determined the flow-rate dependent effective charge density, which influences the electrostatic configuration around SWNT devices.

Nanoscale devices based on a platform of one-dimensional (1D) materials such as single-walled carbon nanotubes (SWNTs) and nanowires (NWs) have shown promise for various applications in electronic, optoelectronic, and bio/chemical sensing.<sup>1-4</sup> In particular, field effect transistors (FET) based on semiconducting nanotubes have been found to be very sensitive to their surroundings, because they have a large carrier mobility and the conduction channel with its nanometer diameter is in direct contact with the environment.<sup>5</sup> These devices exhibit a charge-sensitive conductance, which is ideal for electronic detection of chemicals<sup>6-8</sup> and biomolecules<sup>9, 10</sup> in both aqueous and ambient environments.

---

\* Corresponding author. Electronic mail: ahny@ajou.ac.kr

More recently, SWNTs have been employed for the sensitive determination of charge distribution at SiO<sub>2</sub> surfaces in high-purity aqueous solutions.<sup>11</sup>

Another potential application of SWNT devices in aqueous environments is the fabrication of nanoscale fluidic sensors. In a pioneering work by Ghosh et al. a liquid solution flowing along SWNT bundles in a microfluidic channel was found to induce a flow-rate dependent voltage.<sup>12</sup> In addition, fluidic sensors fabricated from individual SWNTs, Si nanowires, and graphene devices have been reported by a number of groups.<sup>13-16</sup> The conductance of FET devices based on these low-dimensional materials changes significantly with the flow rate of aqueous ionic solutions. The streaming potential model has been adopted to explain the change in conductance. Flow sensing studies carried out as a function of ion concentration and flow direction support this model. In Si nanowire and graphene FET devices, it has been found that the sign of the conductance change reverses when the flow direction is switched in accordance with the streaming potential model. However, in the case of SWNTs, whose diameters are less than 1–2 nm, interaction with the surrounding ions can be obscured by the presence of surface charges on the substrate leading to strong screening effects.<sup>11, 17</sup> Therefore, it is highly desirable to develop SWNT flow sensors in which substrate charge effects are suppressed.

In this work, we fabricated nanoscale flow sensors using partially suspended SWNT devices. We found a dramatic (more than tenfold) improvement in sensitivity compared to supported SWNT devices. The sign of the conductance change was independent of flow direction for both supported and suspended SWNT devices. We also determined the flow-rate dependent effective charge density, which influences device conductance.

Flow sensors were prepared from SWNT FET devices using a microfluidic channel (400×100 μm<sup>2</sup> cross section) made with polydimethylsiloxane (PDMS) molds.<sup>13</sup> Fabrication was accomplished using standard photolithography techniques with CVD-grown SWNTs.<sup>18-21</sup> SWNTs were first synthesized directly on a 220-nm thick thermal oxide layer on a conducting Si substrate. The diameter of the nanotubes appears to be less than 2.5 nm, indicating that they are mostly single-walled. Most of FET devices based on CVD-grown SWNTs exhibit semiconducting or quasi-metallic behaviors (due to

curvature-induced bandgap formation) with a clear gate response. Metal evaporation (Cr/Au) and lift-off were used to define the drain (D) and source (S) electrodes. An additional electrode (G) was added on the substrate plane and functioned as a water-gate electrode. To fabricate the partially suspended device, a trench was chemically etched beneath the SWNT at the center of the structure by HF treatment for 180 s followed by treatment with KOH solution.<sup>22</sup> The trench was 1.0–1.2  $\mu\text{m}$  wide and was located between the S and D electrodes, which are 3  $\mu\text{m}$  apart, as shown in the SEM image in Fig. 1a. The depth of trench structure reaches 600–800 nm. A schematic diagram of the apparatus is shown in Fig. 1b. We used a push-pull syringe pump to produce a laminar flow of deionized (DI) water in the microfluidic channel. An external flow sensor (Upchurch Scientific, N-565) was added to the system to measure flow rate as shown in Fig. 1c.

We begin by demonstrating the behavior of a conventional SWNT device without a trench structure. Fig. 2a shows representative flow sensing results using a supported SWNT. The current signal at the SWNT was monitored with the source-drain bias ( $V_{\text{SD}}$ ) maintained at 10 mV while the flow was switched off and on. Water gate bias voltage was fixed at  $V_{\text{wg}} = 0$  V. We used a relatively large flow rate of 200  $\mu\text{L}/\text{min}$  (flow velocity = 83.3 mm/s) and measured a conductance change of 2  $\mu\text{S}$ . This response is consistent with results given in a previous report.<sup>13</sup> The origin of the conductance change has been attributed to the electrochemical streaming potential generated by ionic movement. In the streaming potential model, the conductance change should reverse its sign when the direction of flow is changed. Results with flow sensors fabricated from SiNWs<sup>14</sup> and graphenes<sup>15, 16</sup> (with a relatively large channel width) have shown clear switching behavior upon a change in flow direction. Such behavior has yet to be demonstrated explicitly for SWNTs. Unlike SiNWs, which have diameters greater than 10 nm, the small (1–2 nm) diameter of SWNTs places them almost entirely within the electrical double layer (EDL) of  $\text{SiO}_2$  surface, which typically ranges from 1–10 nm in breadth depending on the ionic concentration of the solution.<sup>17</sup> Therefore, streaming potential effects may be screened by strongly localized charges near the substrate surface.<sup>11</sup>

In Fig. 2b and 2c we show the DC conductance as a function of gate bias voltage at different flow rates. The plots illustrate the conductance change observed for opposite upstream (SWNT to reference

electrode) and downstream (reference electrode to SWNT) flow directions. In the upstream configuration (Fig. 2b) the conductance minimum shifts towards positive bias by about 190 mV at 100  $\mu\text{L}/\text{min}$  (red line). Therefore, if conductance was monitored at a fixed gate bias voltage, e.g., at  $V_{\text{wg}} = 0$  V, its value should increase with increasing flow as evident from Fig. 2a. As flow rate is further increased, the amount of shift also increases (blue line). The gate potential change per unit flow velocity ( $\alpha = \Delta V_{\text{wg}} / v$ ) is estimated to be 5.45 mV s/mm, which is close to the value reported previously for a SWNT flow sensor.<sup>13</sup>

The results for the downstream mode are illustrated in Fig. 2c. To our surprise, the flow direction did not influence the sign of the conductance change. In other words, the conductance minimum still shifted to positive bias as in the case of upstream flow. All samples (more than 20 including those for which time response only as shown in Fig. 2a was performed) demonstrated only positive shifts, regardless of the direction of flow. The magnitude of the shift varied for the different flow directions. However, we believe this is due to local variation of the fluid velocity, which is easily affected by flow direction. Our results strongly suggest that the streaming potential model is not valid for SWNT flow sensors. Instead, it is more likely that the conductance change is due to the flow-induced depletion of ions, which interact electrostatically with the SWNT (Fig. 2d). The principal mechanisms for SWNT sensing of biological and chemical specimens have been attributed mainly to electrostatic gating effects arising from the addition or depletion of surrounding charges.<sup>5, 10, 11</sup> In our case cations in the diffuse layer of the EDL are loosely bound to the surface. Therefore, part of them can be swept away to an extent that depends on the strength of the water flow, which reduces the equilibrium charge density near the SWNT. The decreased population of cations near the SWNT should result in a shift to positive bias, which is consistent with our results including the fact that the conductivity change is independent of flow direction.

We now discuss results for the partially suspended SWNT devices that are illustrated in Fig. 1. Fig. 3a shows the conductance measured as function of time as the flow of water is turned on and off and the flow rate is varied from 1–7  $\mu\text{L}/\text{min}$  (with  $V_{\text{SD}} = 10$  mV and  $V_{\text{wg}} = 0$  V). We found that the sensitivity increases dramatically when employing the partially suspended SWNT device; in other words, an

equivalent change in conductance is observed at a much lower flow rate. For example, a conductivity change of 250 nS is observed at a flow rate of 1  $\mu\text{L}/\text{min}$  (0.42 mm/s). The conductance change increases gradually until it saturates at 1.86  $\mu\text{S}$  at a flow rate of 5  $\mu\text{L}/\text{min}$  (2.08 mm/s) as shown in Fig. 3b. The time-traces recorded at a fixed  $V_{\text{wg}} = 0$  V show a saturation behavior that originates from device conductance saturation, as will be shown below. In addition, we found that the time response of SWNT device was improved dramatically if we passivate the metal surface with insulating materials such as  $\text{SiO}_2$  (Supplementary information S1).

Fig. 4a illustrates the change in DC conductance as a function of gate bias at different flow rates for another partially suspended SWNT device. The conductance change shifts toward positive bias as flow rate is increased with much higher sensitivity than the supported case. The gate shift is linearly dependent on water flow rate as shown in Fig. 4b. In this example  $\alpha$  is estimated to be 97.15 mV s/mm, which is the maximum result among our experiments and is 20 times higher than the average value for supported devices (*vide infra*). If  $\Delta G$  is monitored at  $V_{\text{wg}} = 0$  V,  $\Delta G$  should increase with increasing flow, whereas the saturation behavior occurs (as found in Fig. 3) due to the saturation of the turn-on conductance even when  $\Delta V_{\text{wg}}$  increases linearly with the flow rate. We also note that  $\Delta V_{\text{wg}}$  change exhibits only positive values regardless of the direction of water flow as observed for supported SWNTs (Supplementary information S2). In addition,  $\Delta V_{\text{wg}}$  did not change significantly with gate sweep direction for devices we tested (Supplementary information S3).

The increased sensitivity of suspended SWNT devices can be explained within the scope of the ion depletion model that we introduced earlier as a plausible mechanism for flow sensing with supported SWNTs. In other words, the SWNT senses the change in the cation distribution in the diffuse layer, whose equilibrium profile is determined by the flow velocity. As mentioned above, the electrostatic interaction of supported SWNTs tends to be obscured by the strong negative charges on the underlying  $\text{SiO}_2$  surface. However, for the unsupported part of a suspended SWNT the charge distribution is free from substrate charges, and the EDL is established cylindrically about the SWNT. Since the suspended part of SWNT has an electrical contact with the parts supported on  $\text{SiO}_2$ , the SWNT will be surrounded by effective cations. In this case cations in the diffuse layer tend to be swept away more efficiently by

the water flow, and, importantly, the SWNT will experience a more significant change in electrostatic environment due to the increased volume of surrounding solution relative to the supported case.

The linear charge density,  $q_{eff}$ , which is responsible for the change of conductance can be extracted from the gate shift,  $\Delta V_{wg}$ , and the relation  $q_{eff} = C_Q \Delta V_{wg}$ , where  $C_Q$  is the SWNT's quantum capacitance ( $C_Q = 4e^2 / \pi \hbar v_F = 4 \times 10^{-10}$  F/m).<sup>23-26</sup> We obtain a charge density of  $\sim 1200 e \mu\text{m}^{-1}$  at a flow rate of 10  $\mu\text{L}/\text{min}$  (see right-hand axis of Fig. 4(b)) compared to the case of supported SWNTs, which require more than 100  $\mu\text{L}/\text{min}$  to achieve a comparable value.  $q_{eff}$  is the quantity that influences the electronic band structure in the SWNT and, thus, is termed the effective charge density. The effective charge density responsible for  $\Delta V_{wg}$  is in a reasonable agreement with those surrounding the supported SWNT devices, measured using a scanning photocurrent microscopy recently, whereas the detailed charge configuration on the suspended SWNTs has to be investigated further.<sup>11</sup> As shown schematically in Fig. 4c, we believe that the large conductance change originates from the complete exposure of the suspended part of the SWNT to water flow without hindrance from substrate charges. The electron energy band will be shifted upward upon the depletion of cations as schematically illustrated in Fig. 4d. It is clear that the suspended part will suffer more dramatic change, yet inducing the electrostatic gating effects over the entire devices.<sup>10</sup> In addition, we note that the streaming potential model cannot successfully explain the enhanced sensitivity of suspended SWNT devices. In the streaming potential model, a potential difference is established between the reference electrode and the SWNT due to the flow of excess charges that are swept from the diffuse layer at the  $\text{SiO}_2$  surface, which is not appropriate to explain the enhancement. We would like to note that reduced viscous resistance due to the removal of the  $\text{SiO}_2$  layer will also increase the sensitivity, resulting in the increase of the local flow velocity. We believe this is very interesting issue that has to be addressed in more detail in future investigations.

Finally, we compare the sensitivity of suspended and supported SWNT devices in Table 1. The sensitivity varies depending on the device conductance, gate response, and possibly position in the fluidic channel. We measured 10 and 6 devices employing suspended and supported SWNTs, respectively, and determined the average values of  $\alpha$ . For comparison, we also appended results found in

the literature for nanoscale FET devices with SWNTs, graphenes, and Si NWs. The average value of  $\alpha$  of 4.25 for our supported SWNTs is very close to that of previous work with SWNT, graphene, and Si NW devices. However, we determined an average  $\alpha$  value of 47.49 (with a maximum result of 97.15) for suspended SWNT devices, which is more than 10 times greater than that of any nanoscale FET device reported to date. In general, there is a large sample-to-sample variation in SWNT device performance, influenced by various factors such as nanotube chirality, metal contacts, defects, surface-induced deformations, and chemical environments. Since these influence the electrostatic gating, their correlation to the sensitivity of SWNT fluidic devices can be a very interesting issue. For example, quasi-metallic SWNT shows better sensitivity than that of semiconducting one for the devices we tested, which is likely due to the relatively low quantum capacitance of low band-gap materials.<sup>27</sup> We believe that the sensitivity can be further improved by optimizing the design of the trench structure, for instance, by simply increasing the suspended part of devices.

Table 1. Comparison of the gate potential change per unit flow velocity according to material

Material	$\alpha$ (mV s/mm)	Reference
SWNT	2.64	13
SiNW	3.9	14
Graphene	2.43	15
Supported SWNT	4.25	this work
Suspended SWNT (our maximum result)	47.49 (97.15)	this work

In summary, we have fabricated highly sensitive flow sensors using suspended SWNTs in aqueous environments. We achieved an enhanced sensitivity (gate potential change per unit flow velocity) of more than one order of magnitude for suspended SWNT devices compared to that of devices employing supported SWNTs and other low-dimensional materials such as Si NWs and graphenes. We also found that the streaming potential model is not applicable to SWNT flow sensors in both supported and suspended configurations. Rather, a reduction in cation density in the diffuse part of the electrical double

layer surrounding the SWNT is responsible for the flow-dependent conductance change. We also measured the linear charge density, which is responsible for the SWNT conductance change. Although we have demonstrated an unprecedented sensitivity for liquid flow sensing, we believe suspended SWNT devices hold great potential as biological and chemical detectors based on their enhanced sensitivity.

## **ACKNOWLEDGMENTS**

This work was supported by the Midcareer Researcher Program (2014R1A2A1A11052108) and PRC Program (2009-0094046), and Public Welfare & Safety Research Program (2011-0020819) through a National Research Foundation grant funded by the Korea Government (MSIP).

## FIGURE CAPTIONS

Fig. 1 (a) SEM image of a partially suspended SWNT device with a trench width of 1.1  $\mu\text{m}$ . (b) Schematic illustration of the microfluidic sensor showing the locations of the source (S), drain (D), and water-gate (G) electrodes and the SWNT. The SWNT is located above a PDMS microchannel ( $400 \mu\text{m} \times 100 \mu\text{m}$ ). (c) Schematic diagram of the experimental setup for measuring flow rate.

Fig. 2 Sensing results with a supported SWNT device. (a) Conductance measured at  $V_{\text{SD}} = 10 \text{ mV}$  and  $V_{\text{wg}} = 0\text{V}$  as a function of time with flow switched on and off at a flow rate of  $200 \mu\text{L}/\text{min}$  ( $83.3 \text{ mm}/\text{s}$ ). (b) DC conductance versus gate bias voltage at flow rates of 0, 100, and  $150 \mu\text{L}/\text{min}$  for the upstream condition. (c) As in (b) with flow rates of 0, 100, and  $200 \mu\text{L}/\text{min}$  for the downstream condition. (d) Schematic illustration of the flow dependent ion depletion model for supported SWNT devices (SL, stern layer; DL, diffuse layer).

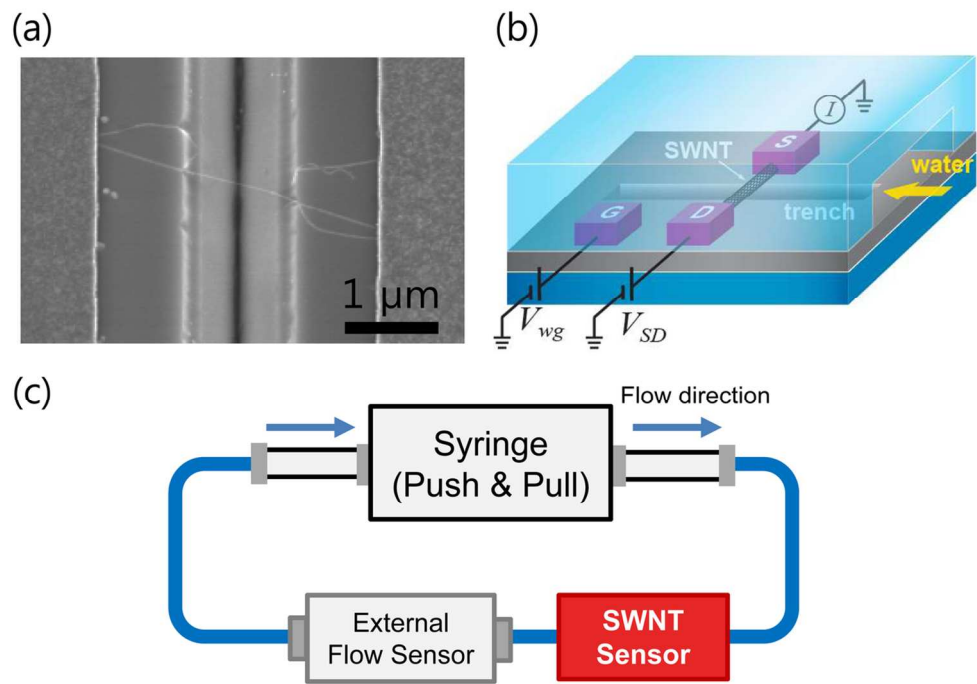
Fig. 3 (a) Conductance as a function of time measured at  $V_{\text{SD}} = 10 \text{ mV}$  and  $V_{\text{wg}} = 0\text{V}$  for a partially suspended SWNT device with flow switched on and off at flow rates of  $1\text{--}7 \mu\text{L}/\text{min}$ . (b) Plot of  $\Delta G$  as a function of flow rate.

Fig. 4 (a) Conductance as a function of  $V_{\text{wg}}$  for a partially suspended SWNT device at flow rates of  $0\text{--}10 \mu\text{L}/\text{min}$  ( $V_{\text{SD}} = 10 \text{ mV}$ ). (b) Plot of  $\Delta V_{\text{wg}}$  (left axis) and the corresponding effective charge density (right axis) as a function of flow rate. (c) Schematic illustration of the flow dependent cation depletion model for suspended SWNT devices. More cations are depleted for the higher flow rate ( $v_1 < v_2$ ). (d) Schematic energy band diagram with (red solid line) and without (blue dotted line) the charge depletion.

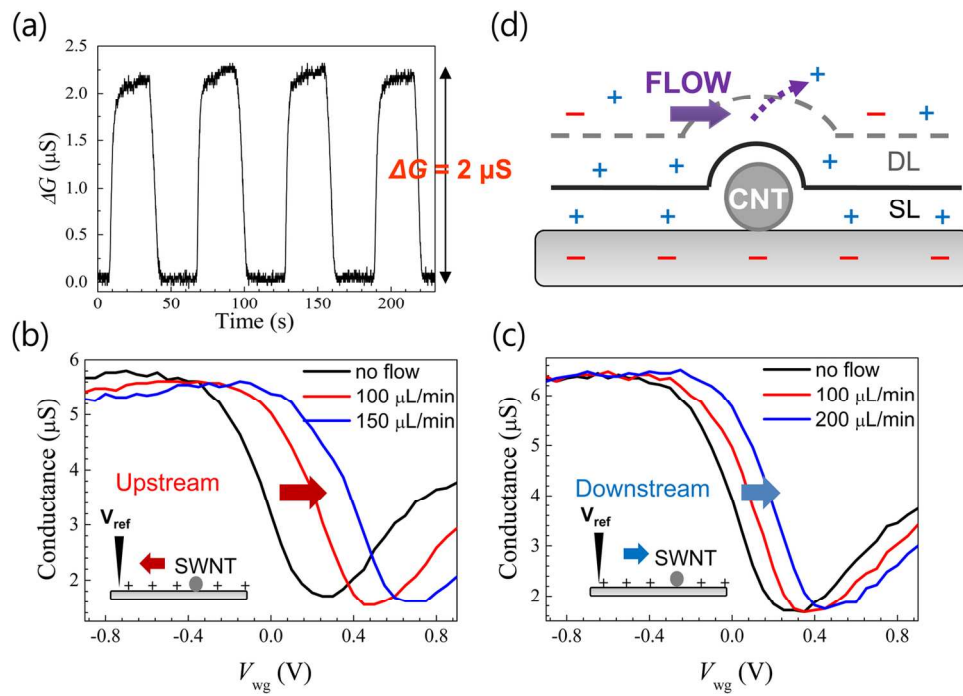
**References**

- 1 P. Avouris, Z. Chen and V. Perebeinos, *Nat. Nanotech.*, 2007, **2**, 605-615.
- 2 C. M. Lieber and Z. L. Wang, *MRS Bull.*, 2007, **32**, 99-108.
- 3 X. Duan, T. M. Fu, J. Liu and C. M. Lieber, *Nano Today*, 2013, **8**, 351-373.
- 4 B. Mahar, C. Laslau, R. Yip and y. Sun, *IEEE Sens. J.*, 2007, **7**, 266-284.
- 5 G. Gruner, *Anal. Bioanal. Chem.*, 2006, **384**, 322-335.
- 6 J. Kong, N. R. Franklin, C. Zhou, M. G. Chapline, S. Peng, K. Cho and H. Dai, *Science*, 2000, **287**, 622-625.
- 7 T. Zhang, S. Mubeen, N. V. Myung and M. A. Deshusses, *Nanotechnology*, 2008, **19**.
- 8 M. Zhang, L. L. Brooks, N. Chartuprayoon, W. Bosze, Y. H. Choa and N. V. Myung, *ACS Applied Materials and Interfaces*, 2014, **6**, 319-326.
- 9 J. N. Tey, I. P. M. Wijaya, J. Wei, I. Rodriguez and S. G. Mhaisalkar, *Microfluid. Nanofluidics*, 2010, **9**, 1185-1214.
- 10 I. Heller, A. M. Janssens, J. Männik, E. D. Minot, S. G. Lemay and C. Dekker, *Nano Lett.*, 2008, **8**, 591-595.
- 11 J. K. Park, B. H. Son, J.-Y. Park, S. Lee and Y. H. Ahn, *Appl. Phys. Lett.*, 2014, **105**, 223101.
- 12 S. Ghosh, A. K. Sood and N. Kumar, *Science*, 2003, **299**, 1042-1044.
- 13 B. Bourlon, J. Wong, C. Mikó, L. Forró and M. Bockrath, *Nat. Nanotech.*, 2007, **2**, 104-107.
- 14 D. R. Kim, C. H. Lee and X. Zheng, *Nano Lett.*, 2009, **9**, 1984-1988.
- 15 R. X. He, P. Lin, Z. K. Liu, H. W. Zhu, X. Z. Zhao, H. L. Chan and F. Yan, *Nano Lett.*, 2012, **12**, 1404-1409.
- 16 A. K. M. Newaz, D. A. Markov, D. Prasai and K. I. Bolotin, *Nano Lett.*, 2012, **12**, 2931-2935.
- 17 E. Stern, R. Wagner, F. J. Sigworth, R. Breaker, T. M. Fahmy and M. A. Reed, *Nano Lett.*, 2007, **7**, 3405-3409.
- 18 Y. H. Ahn, A. W. Tsen, B. Kim, Y. W. Park and J. Park, *Nano Lett.*, 2007, **7**, 3320-3323.

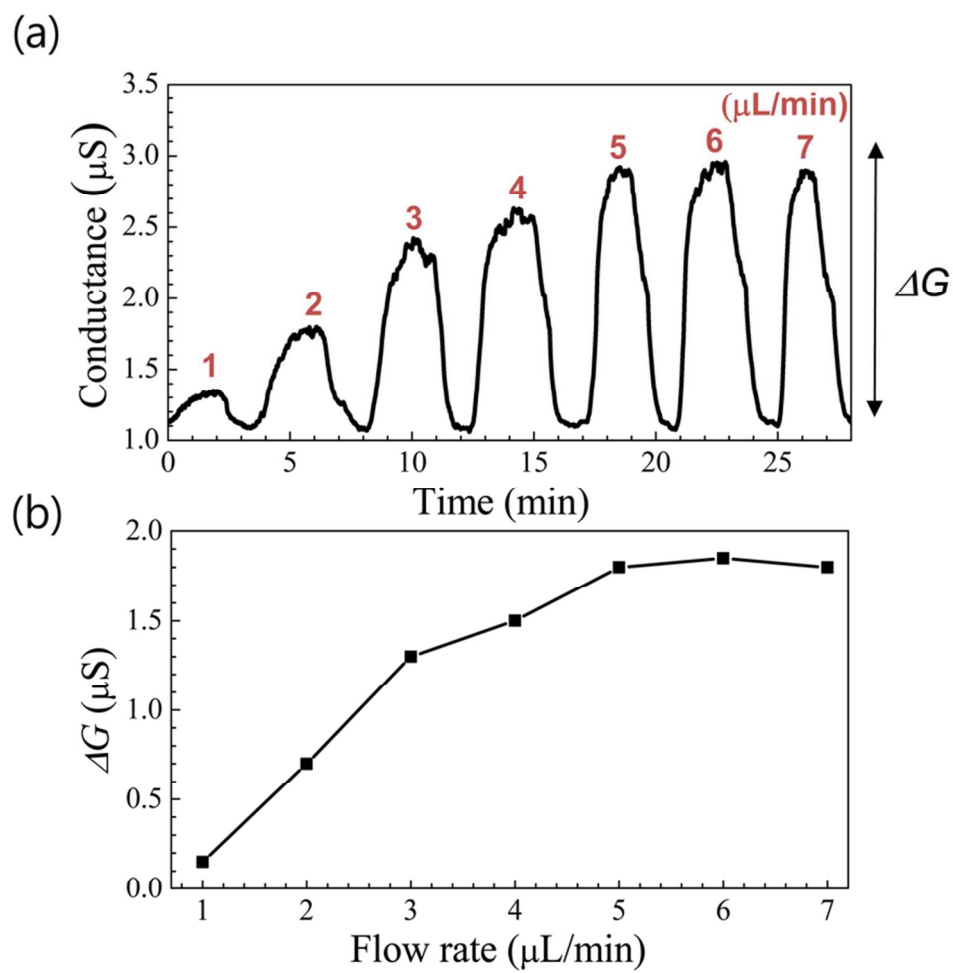
- 19 J.-Y. park, *Appl. Phys. Lett.*, 2007, **90**, 023112.
- 20 Q. N. Thanh, H. Jeong, J. Kim, J. W. Kevek, Y. H. Ahn, S. Lee, E. D. Minot and J. Y. Park, *Adv. Mater.*, 2012, **24**, 4499-4504.
- 21 B. H. Son, J. K. Park, J. T. Hong, J. Y. Park, S. Lee and Y. H. Ahn, *ACS Nano*, 2014, **8**, 11361-11368.
- 22 J. K. Park, Y. H. Ahn, J. Y. Park, S. Lee and K. H. Park, *Nanotechnology*, 2010, **21** 115706.
- 23 K. Bradley, M. Briman, A. Star and G. Gruner, *Nano Lett.*, 2004, **4**, 253-256.
- 24 M. T. Martínez, Y. C. Tseng, N. Ormategui, I. Loinaz, R. Eritja and J. Bokor, *Nano Lett.*, 2009, **9**, 530-536.
- 25 N. Peng, Q. Zhang, C. L. Chow, O. K. Tan and N. Marzari, *Nano Lett.*, 2009, **9**, 1626-1630.
- 26 S. Rosenblatt, Y. Yaish, J. Park, J. Gore, V. Sazonova and P. L. McEuen, *Nano Lett.*, 2002, **2**, 869-872.
- 27 J. Dai, J. Li, H. Zeng and X. Cui, *Appl. Phys. Lett.*, 2009, **94** 093114.



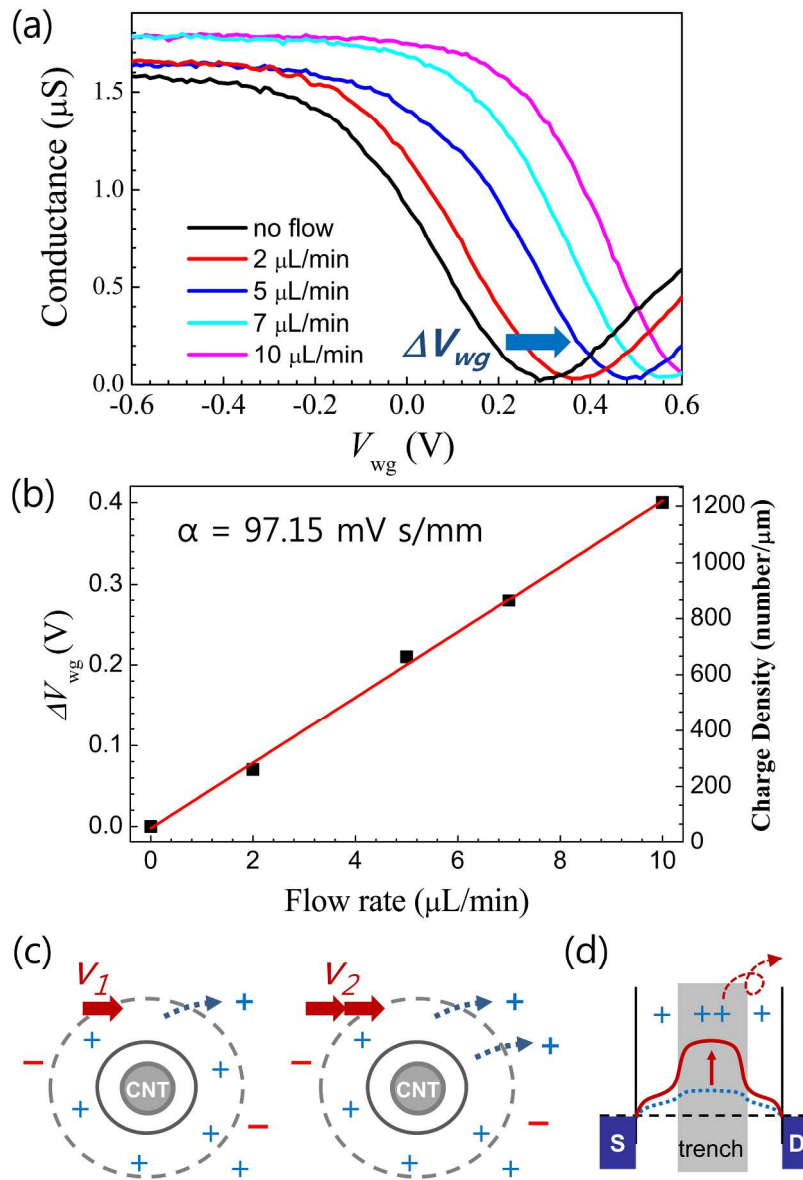
120x86mm (300 x 300 DPI)



140x98mm (300 x 300 DPI)



78x76mm (300 x 300 DPI)



237x333mm (300 x 300 DPI)